The Status of Our Search for Gravitational Waves

Rainer Weiss for the LSC

Tanner Fest

April 22, 2005

University of Florida@Gainesville

Direct detection of gravitational waves from astrophysical sources

- Physics
  - Observations of gravitation in the strong field, high velocity limit
  - Determination of wave kinematics – polarization and propagation
  - Tests for alternative relativistic gravitational theories
- Astrophysics
  - Measurement of coherent inner dynamics – stellar collapse, pulsar formation….
  - Compact binary coalescence – neutron star/neutron star, black hole/black hole
  - Neutron star equation of state
  - Primeval cosmic spectrum of gravitational waves
- Gravitational wave survey of the universe

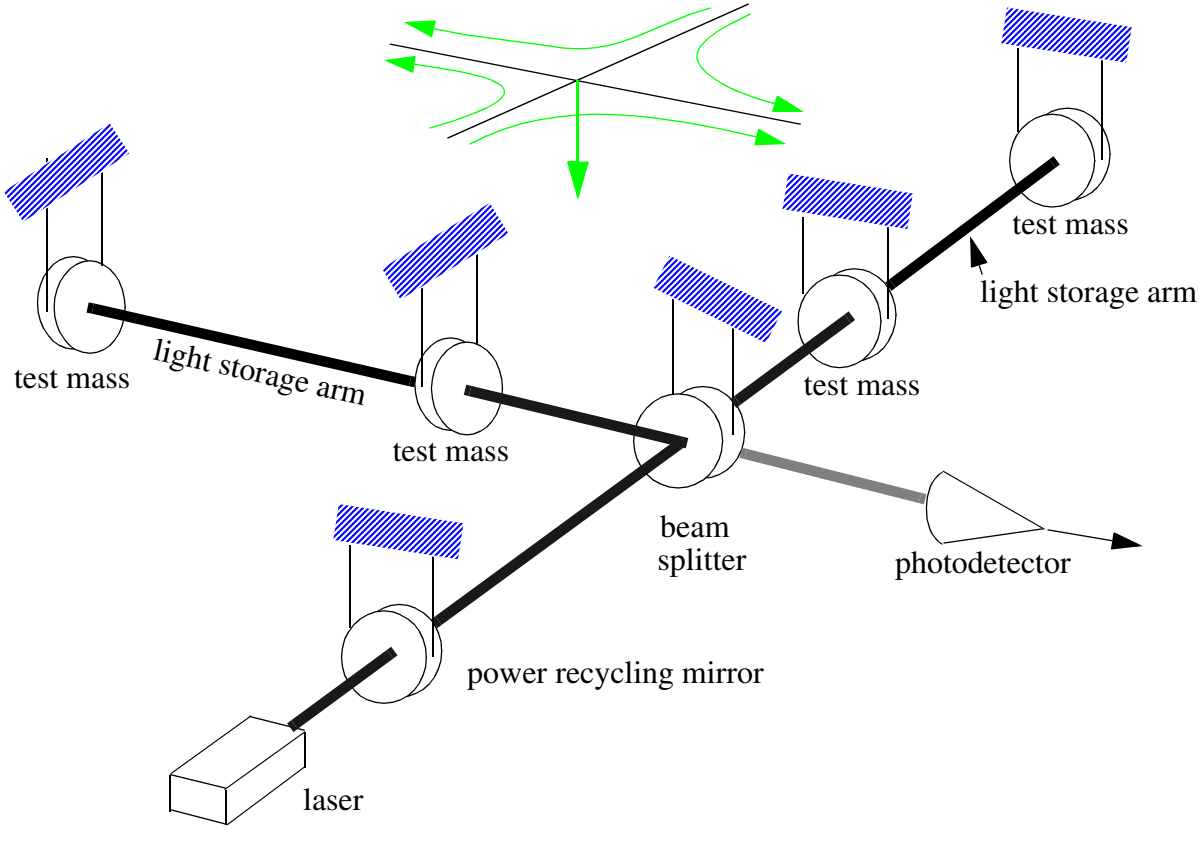
test mass
light storage arm
test mass
test mass
test mass
light storage arm
beam
splitter
photodetector
power recycling mirror
laser

Measurement challenge

- Needed technology development to measure:

$$h = \Delta L/L < 10^{-21}$$

$$\Delta L < 4 \times 10^{-18} \text{ meters}$$

Role of the University of Florida

- Design, construction and installation of the input optics
  - Input mode matching telescope
  - Input mode cleaner
- Development of data analysis techniques
  - Wavelet burst analysis
  - Line removal techniques
- High power optics for Advanced LIGO
- Finding and nurturing Rana Adhikari

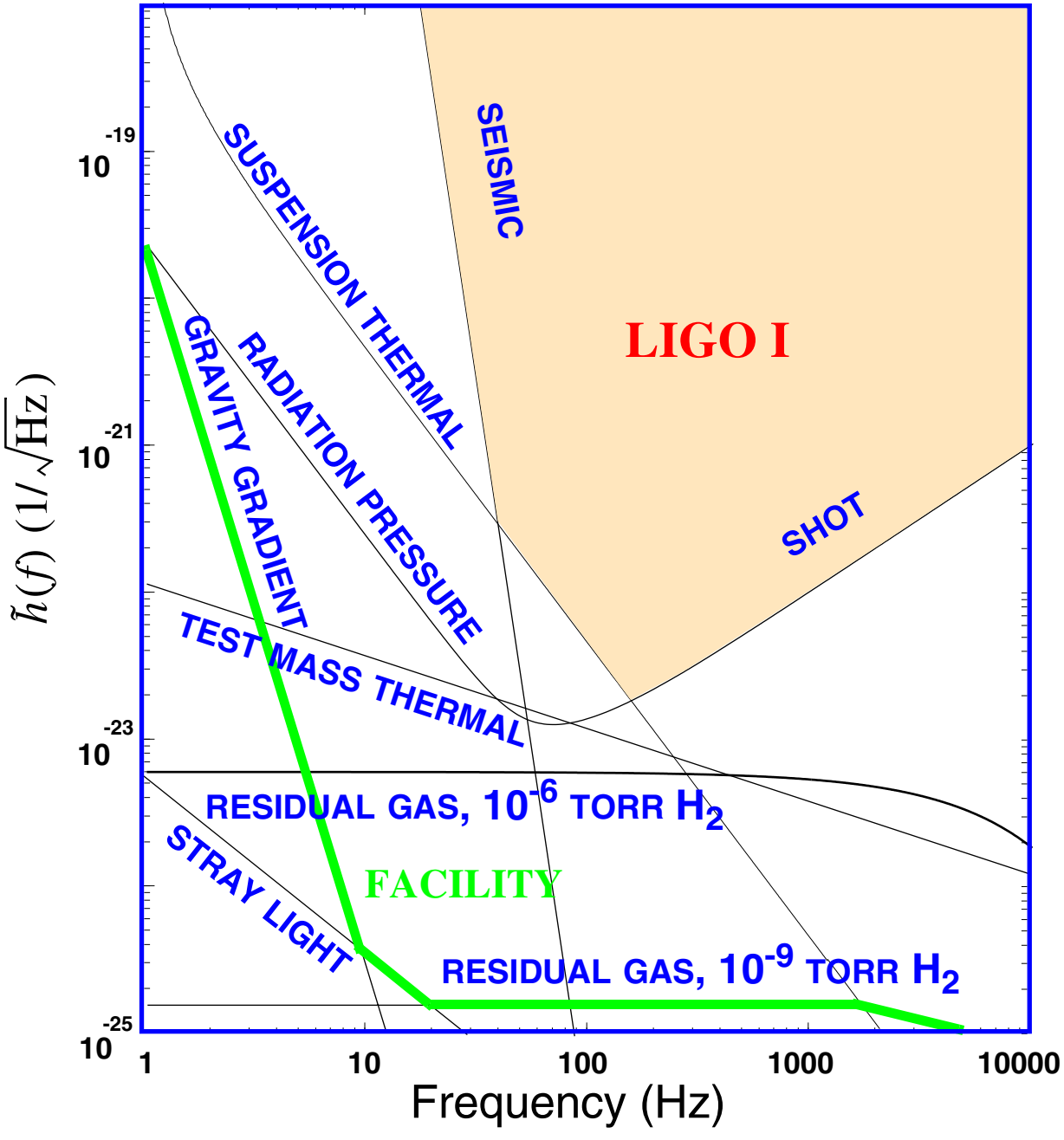
SEISMIC
SUSPENSION THERMAL
RADIATION PRESSURE
GRAVITY GRADIENT
LIGO I
SHOT
TEST MASS THERMAL
RESIDUAL GAS, 10-6 TORR H2
FACILITY
STRAY LIGHT
RESIDUAL GAS, 10-9 TORR H2
10-19
10-21
10-23
10-25
h̃(f) (1/√Hz)
1
10
100
1000
10000
Frequency (Hz)

Interferometers
international network

Simultaneously detect signal (within msec)

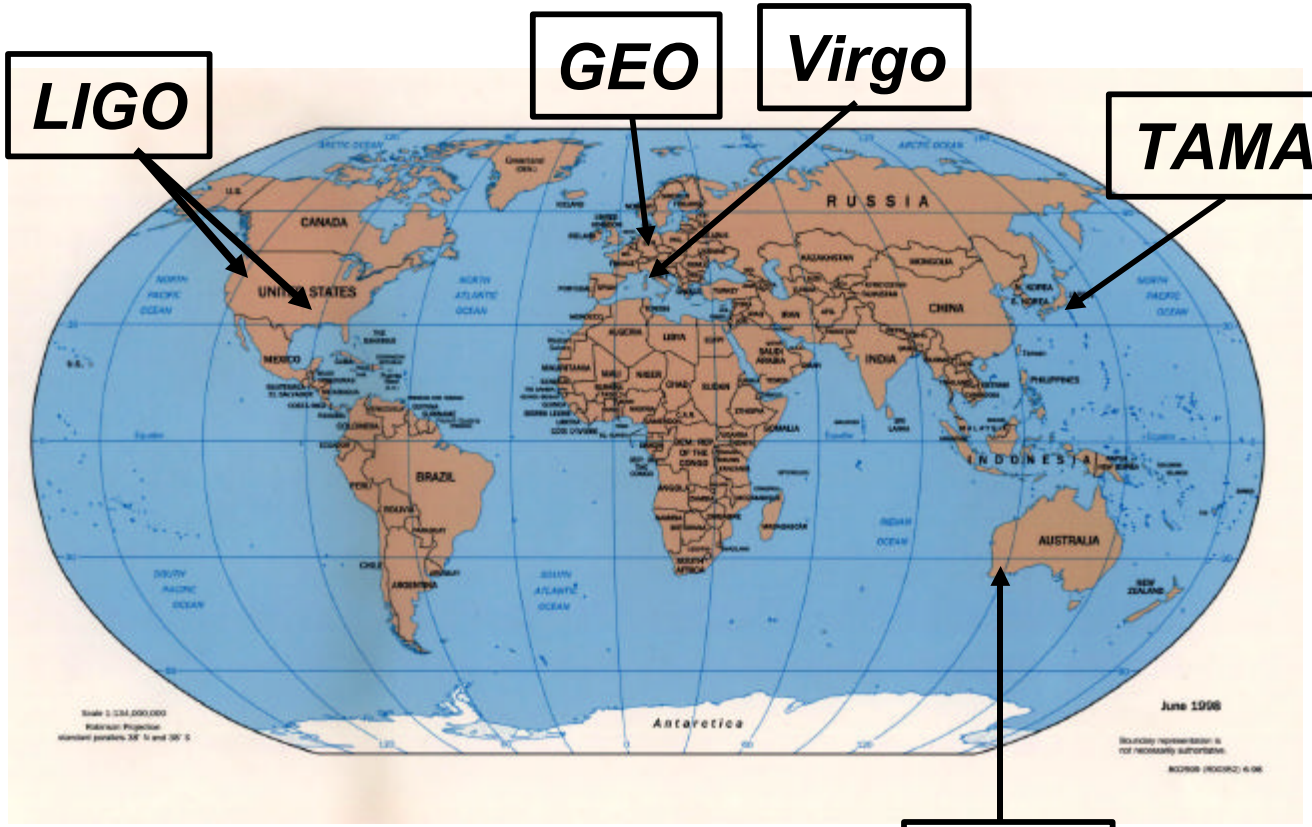

detection confidence

locate the sources

decompose the polarization of gravitational waves

LIGO Observatory Facilities

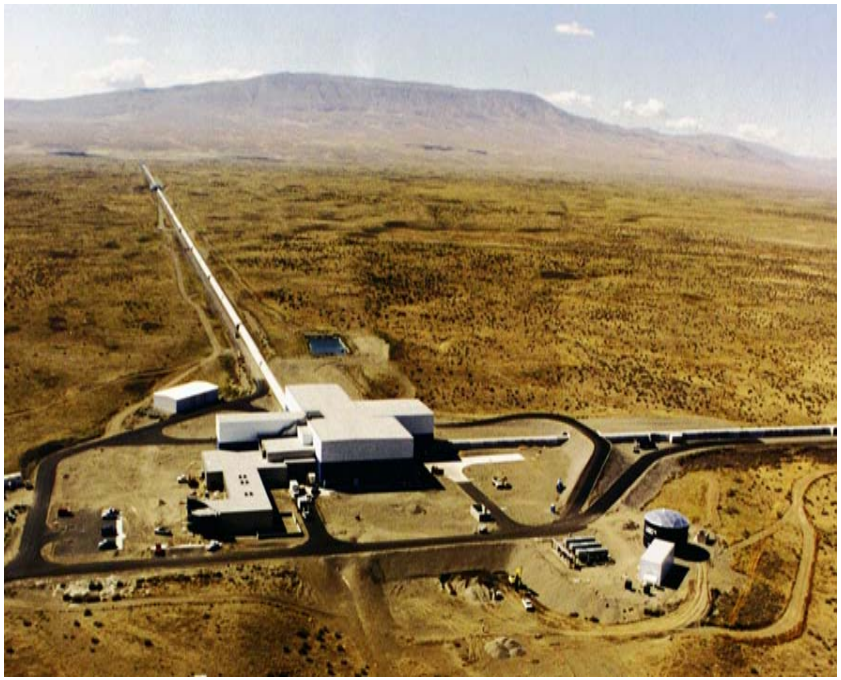

LIGO Hanford Observatory [LHO]

26 km north of Richland, WA

2 km + 4 km interferometers in same vacuum envelope

LIGO Livingston Observatory [LLO]

42 km east of Baton Rouge, LA

Single 4 km interferometer

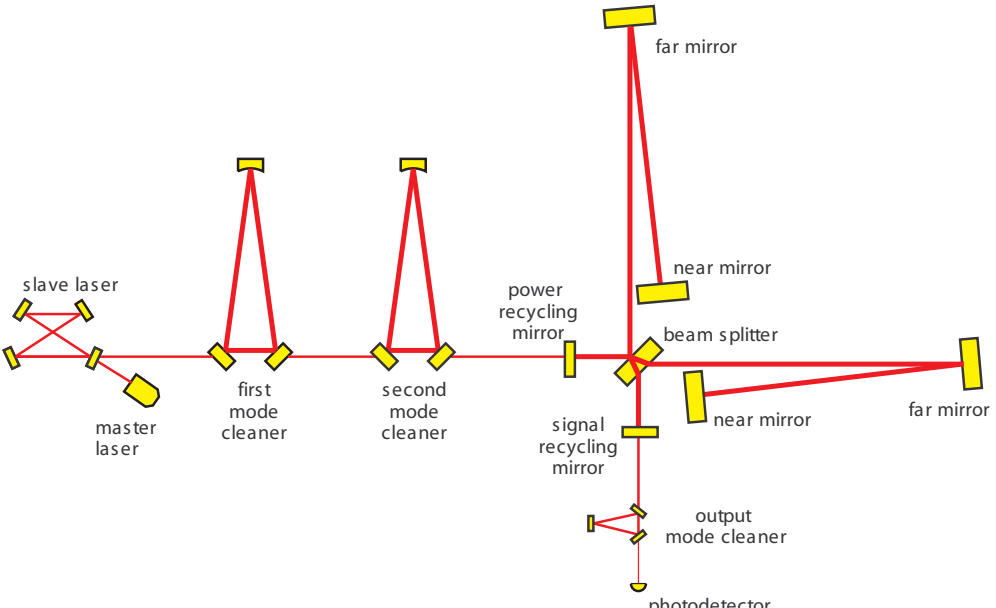
far mirror
near mirror
slave laser
power
recycling
mirror
beam splitter
first
mode
cleaner
second
mode
cleaner
master
laser
near mirror
far mirror
signal
recycling
mirror
output
mode cleaner
photodetector

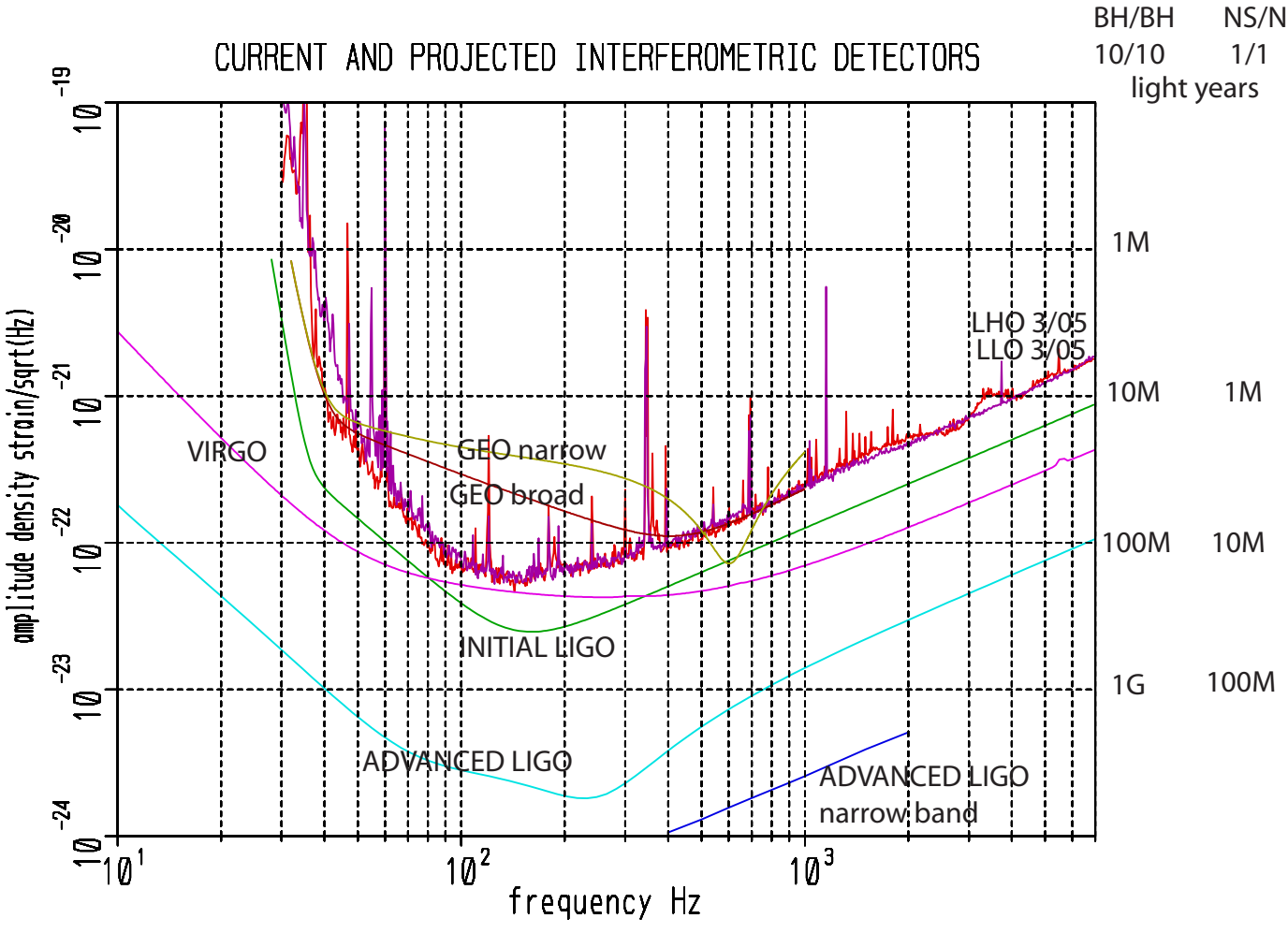
CURRENT AND PROJECTED INTERFEROMETRIC DETECTORS
BH/BH
10/10
NS/NS
1/1
light years
1M
10M
1M
100M
10M
1G
100M
LHO 3/05
LLO 3/05
VIRGO
GEO narrow
GEO broad
INITIAL LIGO
ADVANCED LIGO
ADVANCED LIGO
narrow band
amplitude density strain/sqrt(Hz)
frequency Hz
10^-19
10^-20
10^-21
10^-22
10^-23
10^-24
10^1
10^2
10^3

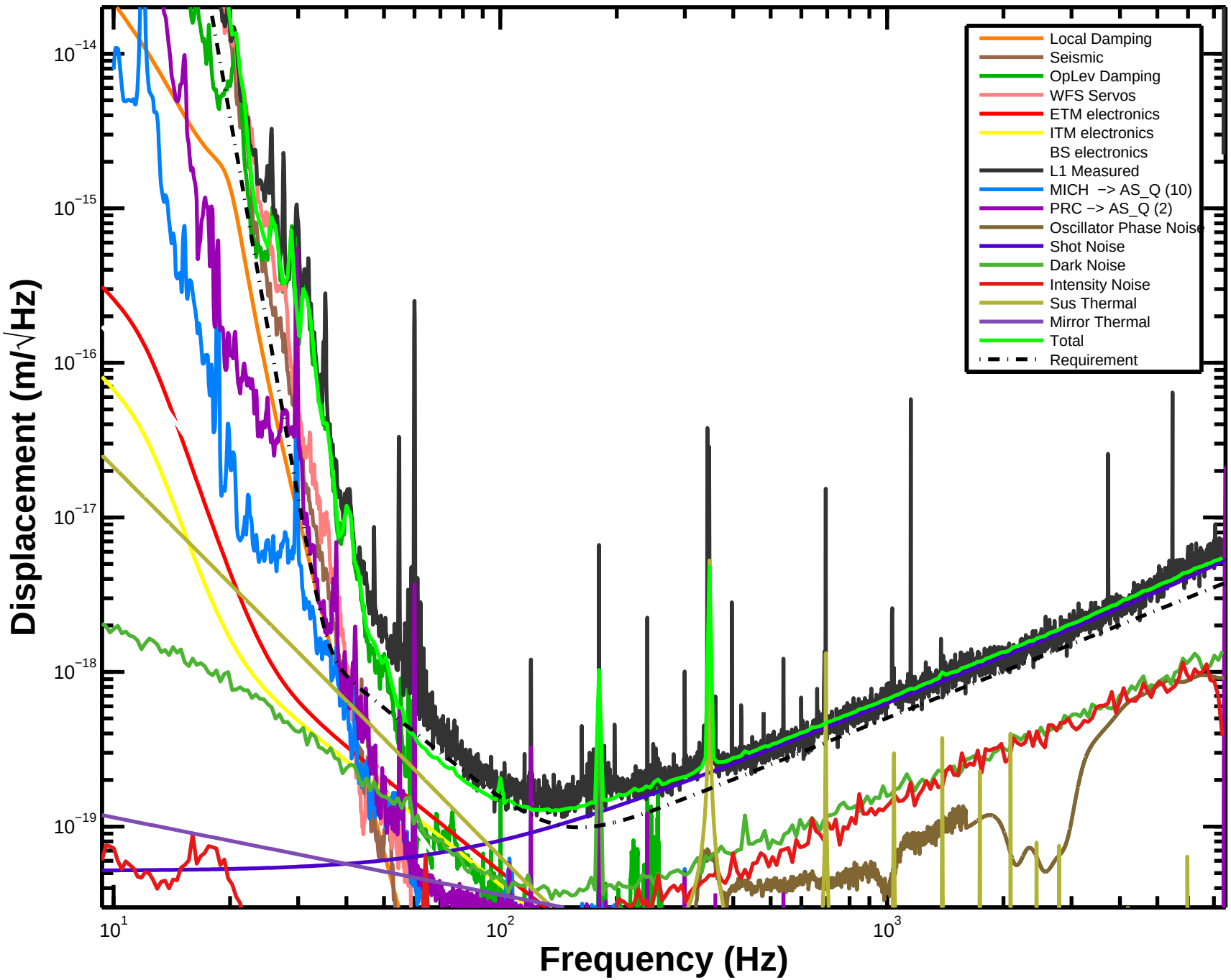
L1: 10.1 Mpc, Apr 20 2005 06:01:38 UTC
Displacement (m/√Hz)
Frequency (Hz)
Local Damping
Seismic
OpLev Damping
WFS Servos
ETM electronics
ITM electronics
BS electronics
L1 Measured
MICH −> AS_Q (10)
PRC −> AS_Q (2)
Oscillator Phase Noise
Shot Noise
Dark Noise
Intensity Noise
Sus Thermal
Mirror Thermal
Total
Requirement

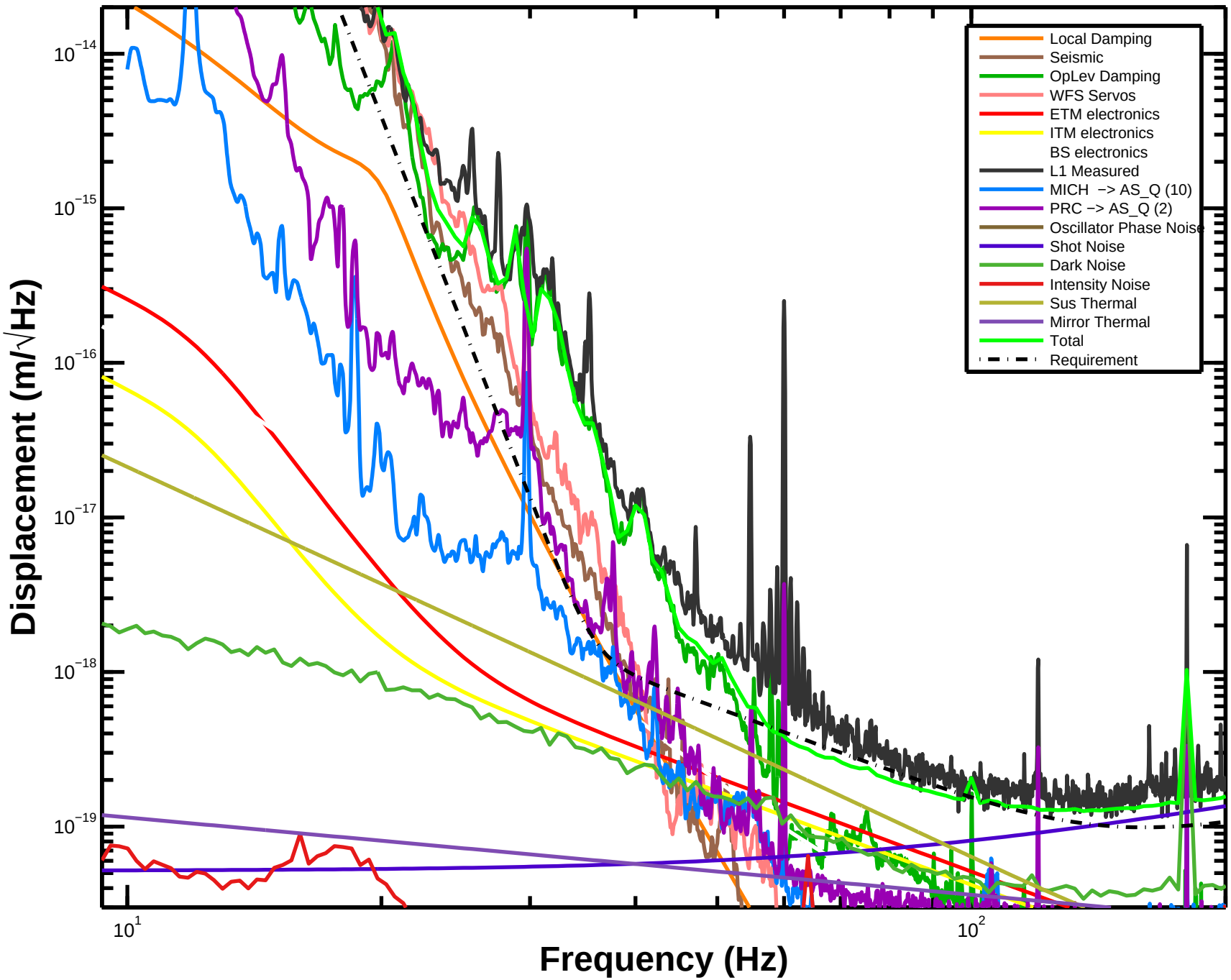
L1: 10.1 Mpc, Apr 20 2005 06:01:38 UTC
Displacement (m/√Hz)
Frequency (Hz)
10^{-14}
10^{-15}
10^{-16}
10^{-17}
10^{-18}
10^{-19}
10^{1}
10^{2}
Local Damping
Seismic
OpLev Damping
WFS Servos
ETM electronics
ITM electronics
BS electronics
L1 Measured
MICH −> AS_Q (10)
PRC −> AS_Q (2)
Oscillator Phase Noise
Shot Noise
Dark Noise
Intensity Noise
Sus Thermal
Mirror Thermal
Total
Requirement

Gravitational Radiation and Detectors:
LIGO Sensitivity Improvements

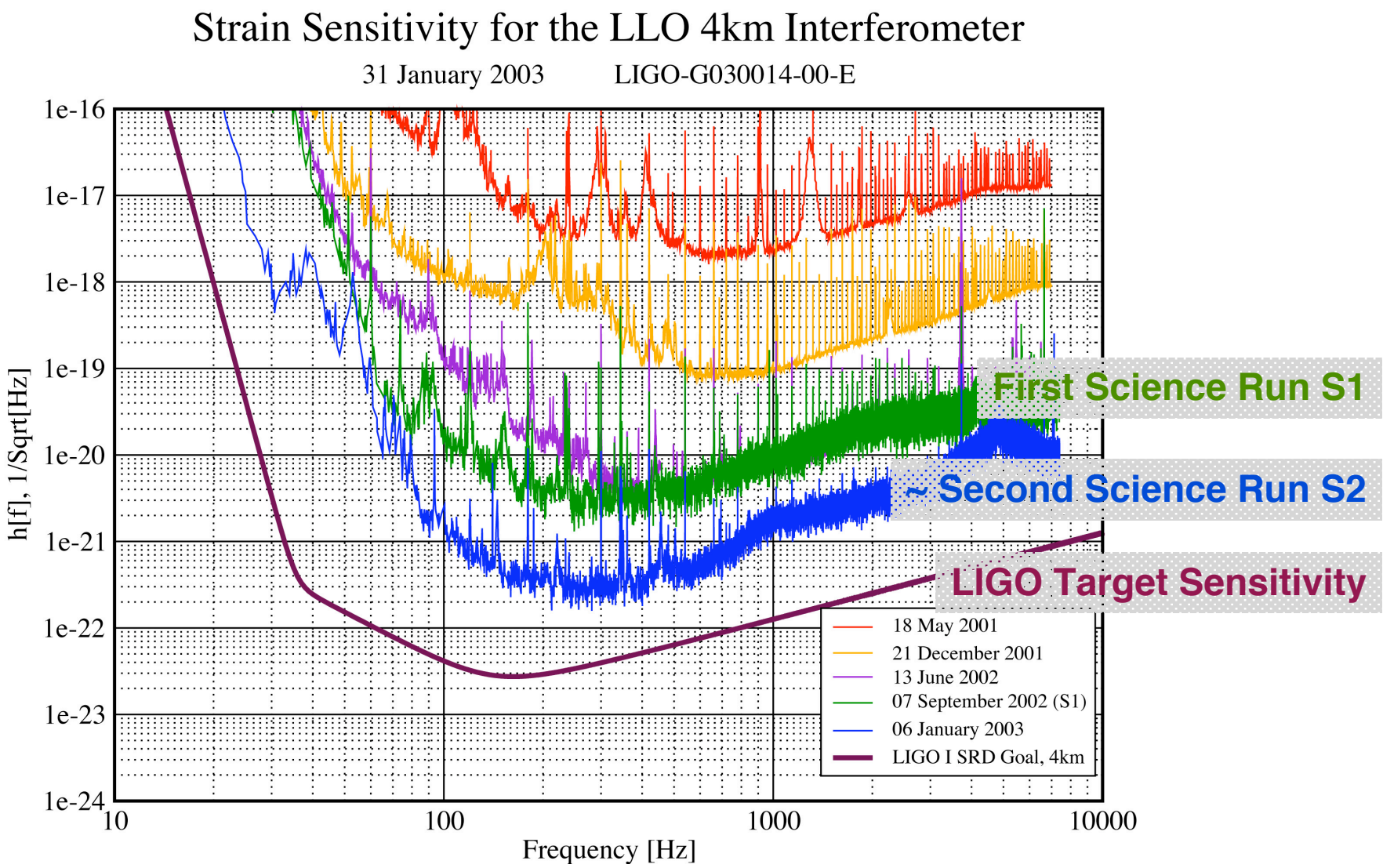

Classes of sources

- Compact binary inspiral: template search
  - BH/BH
  - NS/NS and BH/NS
- Low duty cycle transients: wavelets,T/f clusters
  - Supernova
  - BH normal modes
  - Unknown types of sources
- Periodic CW sources
  - Pulsars
  - Low mass x-ray binaries (quasi periodic)
- Stochastic background
  - Foreground sources : gravitational wave radiometry
  - Cosmological isotropic background

Rate < 47 inspirals/yr/milky way galaxy to a distance of 1.5Mpc
Mass range 1 to 3 solar masses

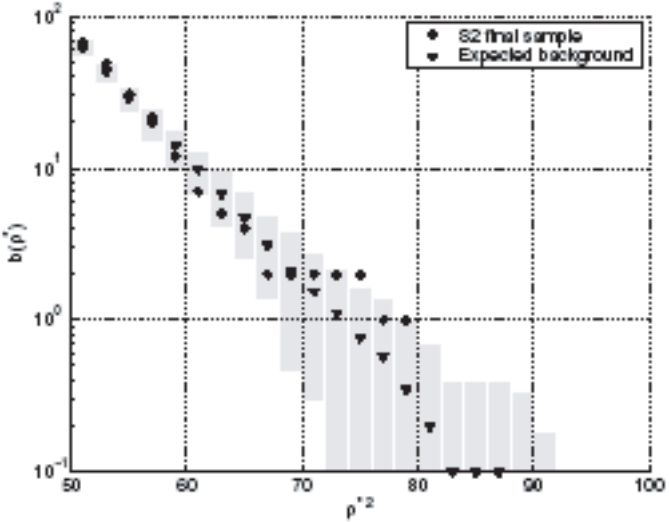

FIG. 10: The mean number of triggers per S2 above SNR ρ^* using the best fit clustering method. The triangles represent the expected background. See Fig. 8 and Sec. VII for details of the time-shifts and for comparison with largest SNR clustering. We note that there is no apparent excess of S2 coincident triggers over the expected background from accidental coincidences in this plot.

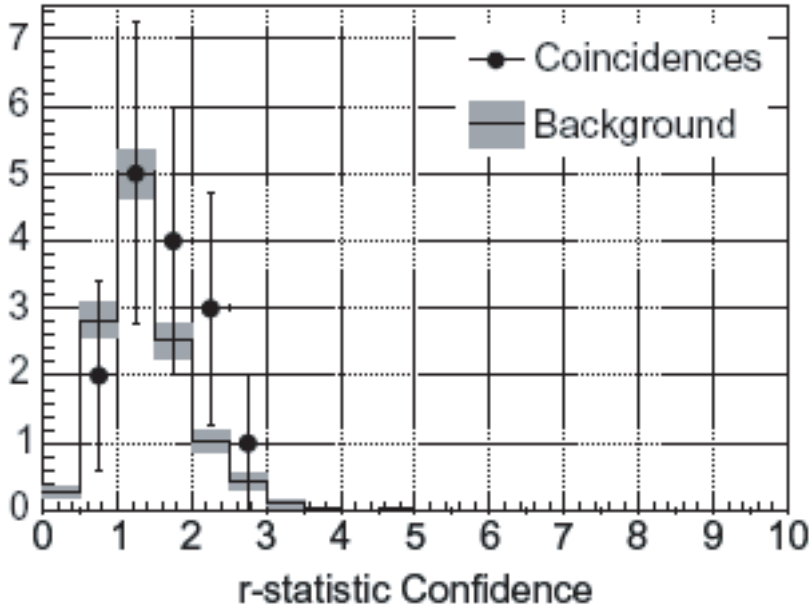

FIG. 7: Histogram of r-statistic confidence values (Γ's), for events passing the WaveBurst analysis at zero-lag (shown with circles) and at time-shifts (*i.e.*, background, shown with bars), after applying the acoustic veto. The histogram of background events is normalized to the live-time of the zero-lag analysis.

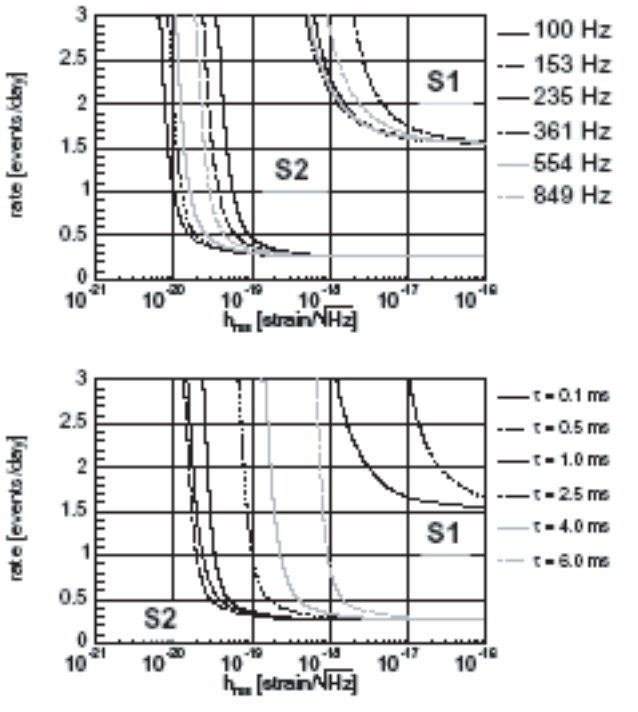

FIG. 12: Rate versus h_{rss} exclusion plots at the 90% confidence level derived from the LIGO burst search using the S2 data. The top plot corresponds to burst events modeled by sine-Gaussians of $Q = 8.9$ and frequencies ranging from 100 Hz to 850 Hz, while the bottom plot corresponds to ones events modeled by Gaussians of the τ's shown. For comparison, the corresponding curves resulting from the S1 analysis are superimposed.

pulsar	spin f (Hz)	spindown $\dot{f}$ (Hz s^{-1})	$h_0^{95\%}$ $/10^{-24}$	ϵ $/10^{-5}$
B0021−72C*	173.71	$+1.50\times10^{-15}$	4.3	16
B0021−72D*	186.65	$+1.19\times10^{-16}$	4.1	14
B0021−72F*	381.16	-9.37×10^{-15}	7.2	5.7
B0021−72G*	247.50	$+2.58\times10^{-15}$	4.1	7.5
B0021−72L*	230.09	$+6.46\times10^{-15}$	2.9	6.1
B0021−72M*	271.99	$+2.84\times10^{-15}$	3.3	5.0
B0021−72N*	327.44	$+2.34\times10^{-15}$	4.0	4.3
J0030+0451	205.53	-4.20×10^{-16}	3.8	0.48
B0531+21*	29.81	-3.74×10^{-10}	41	2 100
J0711−6830	182.12	-4.94×10^{-16}	2.4	1.8
J1024−0719*	193.72	-6.95×10^{-16}	3.9	0.86
B1516+02A	180.06	-1.34×10^{-15}	3.6	21
J1629−6902	166.65	-2.78×10^{-16}	2.3	2.7
J1721−2457	285.99	-4.80×10^{-16}	4.0	1.8
J1730−2304*	123.11	-3.06×10^{-16}	3.1	2.5
J1744−1134*	245.43	-5.40×10^{-16}	5.9	0.83
J1748−2446C	118.54	$+8.52\times10^{-15}$	3.1	24
B1820−30A*	183.82	-1.14×10^{-13}	4.2	24
B1821−24*	327.41	-1.74×10^{-13}	5.6	7.1
J1910−5959B	119.65	$+1.14\times10^{-14}$	2.4	8.5
J1910−5959C	189.49	-7.90×10^{-17}	3.3	4.7
J1910−5959D	110.68	-1.18×10^{-14}	1.7	7.2
J1910−5959E	218.73	$+2.09\times10^{-14}$	7.5	7.9
J1913+1011*	27.85	-2.61×10^{-12}	51	6 900
J1939+2134*	641.93	-4.33×10^{-14}	13	2.7
B1951+32*	25.30	-3.74×10^{-12}	48	4 400
J2124−3358*	202.79	-8.45×10^{-16}	3.1	0.45
J2322+2057*	207.97	-4.20×10^{-16}	4.1	1.8

TABLE I: The 28 pulsars targeted in the S2 run, with approximate spin parameters. Pulsars for which radio timing data were taken over the S2 period are starred (*). The right-hand two columns show the 95% upper limit on h_0, based on a coherent analysis using all the S2 data, and corresponding ellipticity values (ϵ, see text). These upper limit values do *not* include the uncertainties due to calibration and to pulsar timing accuracy, which are discussed in the text, nor uncertainties in the pulsar's distance, r.

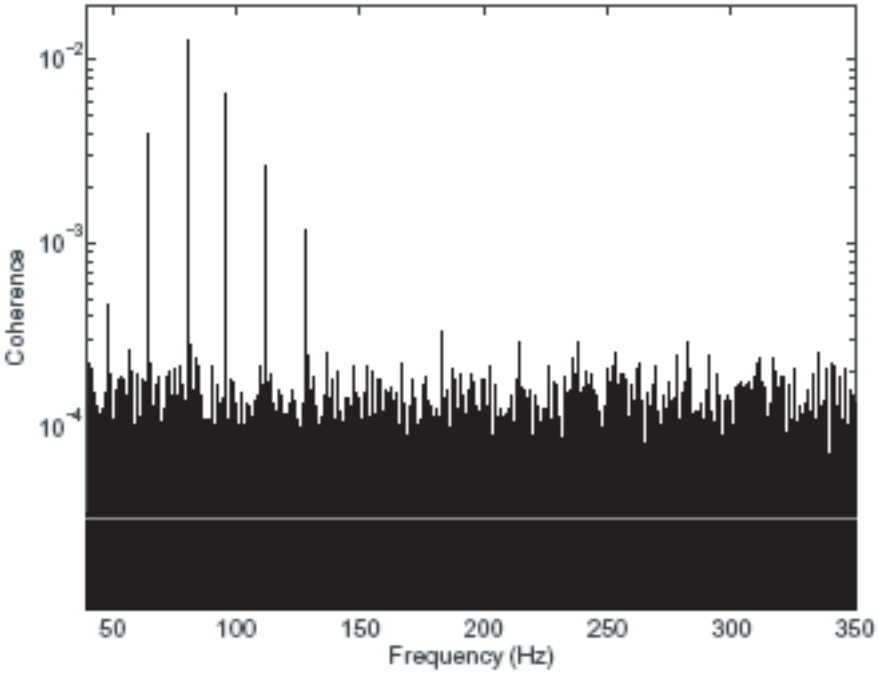

FIG. 2: Coherence between the H1 and L1 detector outputs during S3, showing a few small, but significant, coherent peaks at multiples of 16 Hz. The grey line corresponds to the expected statistical uncertainty level of $1/N_{\rm avg} \approx 3 \times 10^{-5}$.

Overlap reduction function

Specifies the reduction in sensitivity due to the separation and orientation of the two detectors:

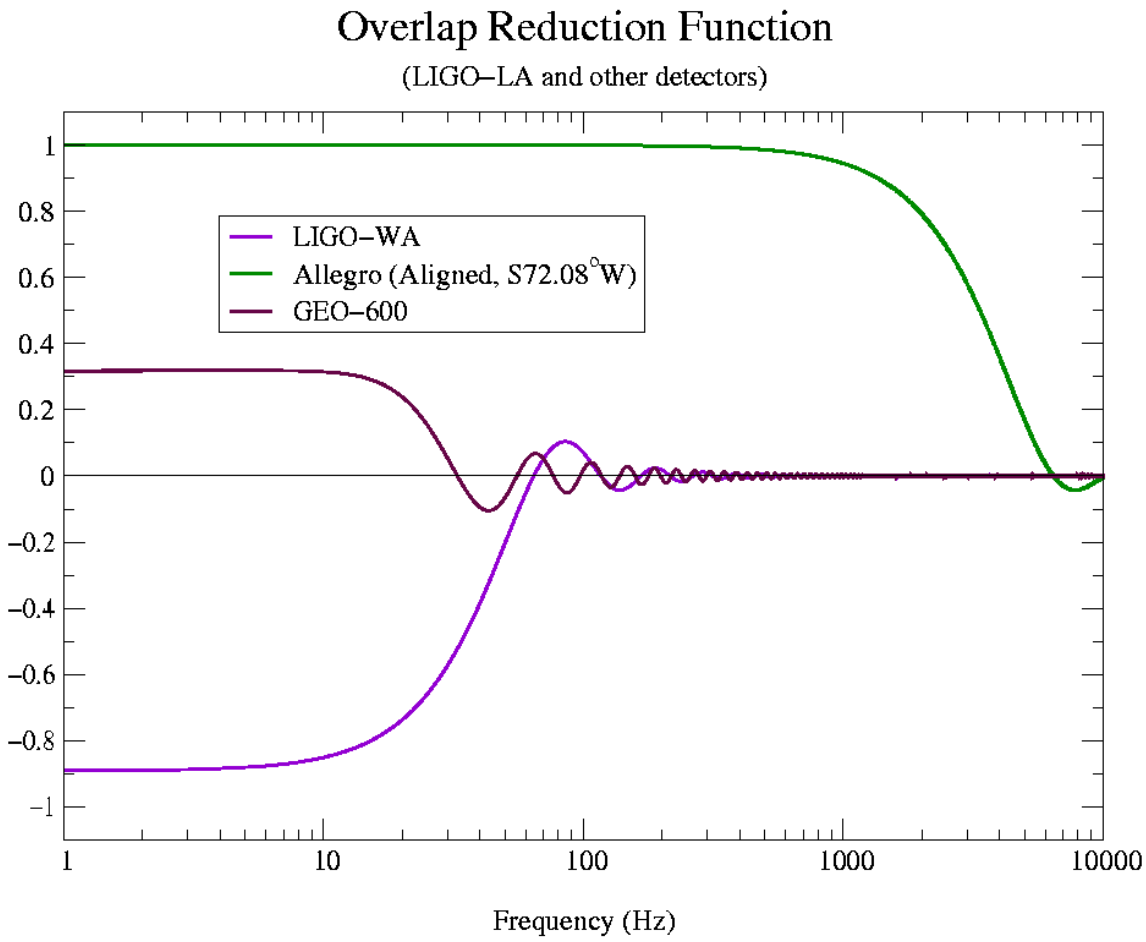

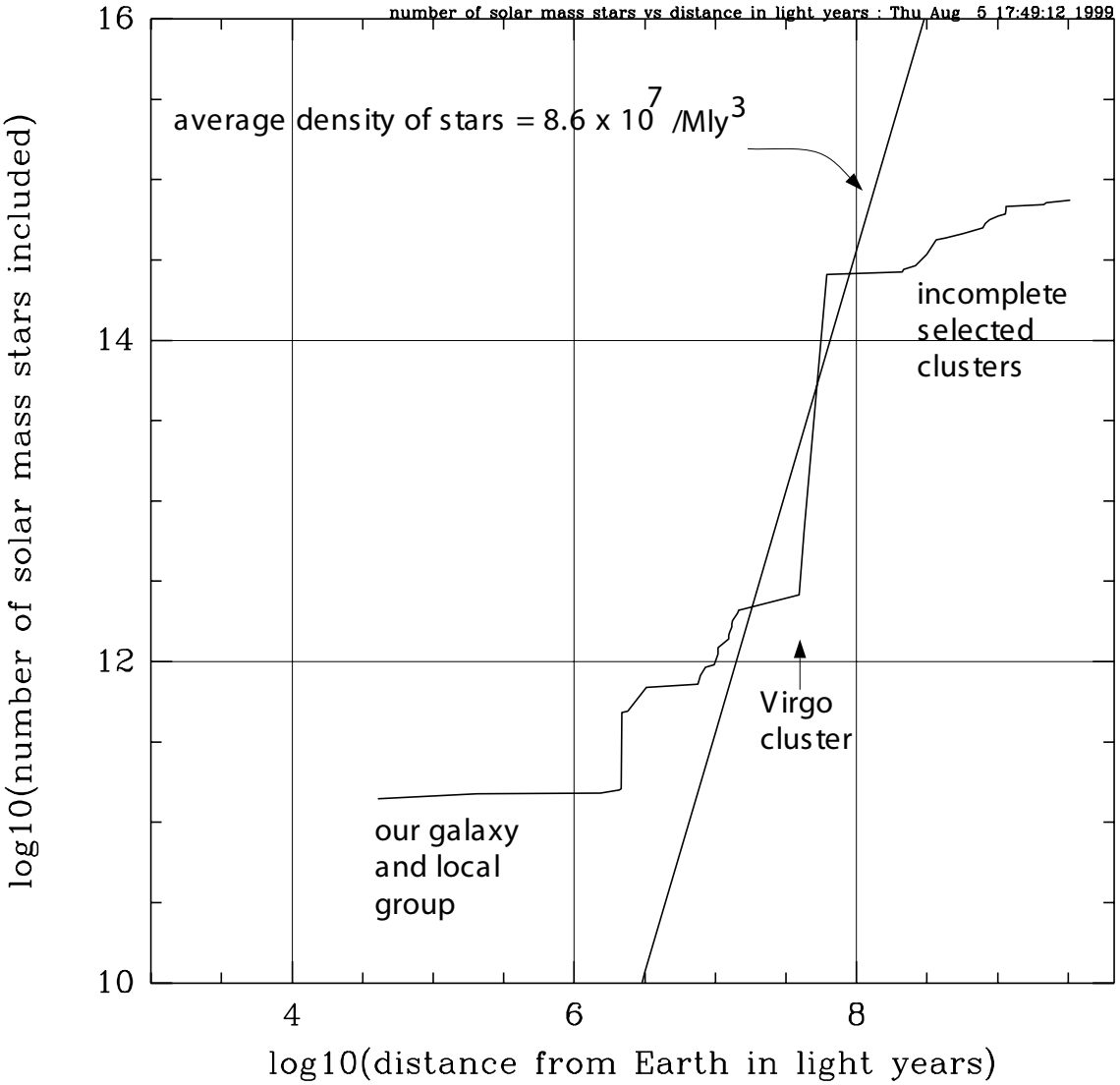

DATA: Cosmology of the Local Group G.Lake
Astrophysical Quantities C.W. Allen

Binary Coalescence Sources & Science:
Binary Neutron Stars: S1 Range

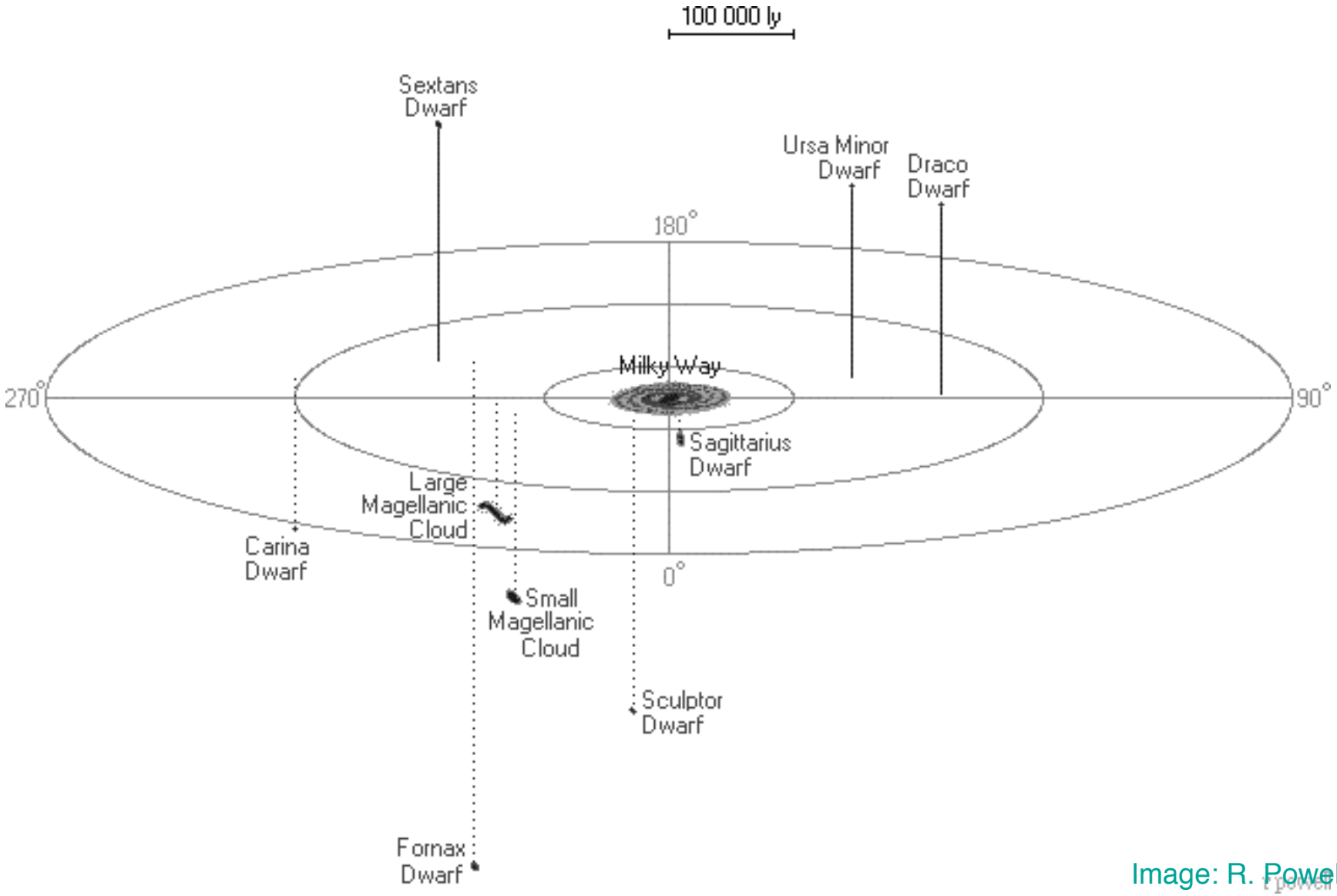

Image: R. Powell

Binary Coalescence Sources & Science:

Binary Neutron Stars: S2 Range

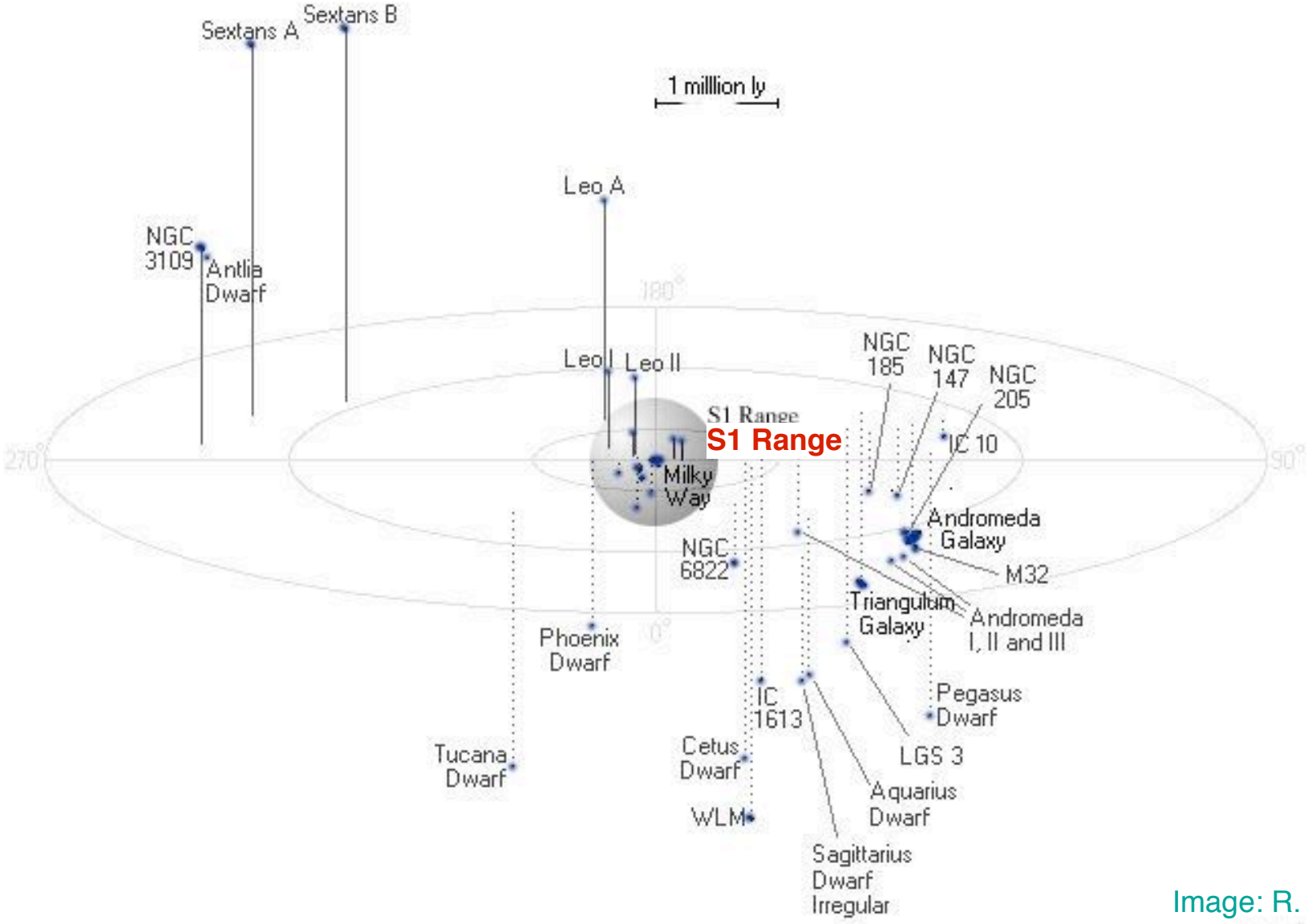

Image: R. Powell

Binary Coalescence Sources & Science:
Binary Neutron Stars: LIGO Range

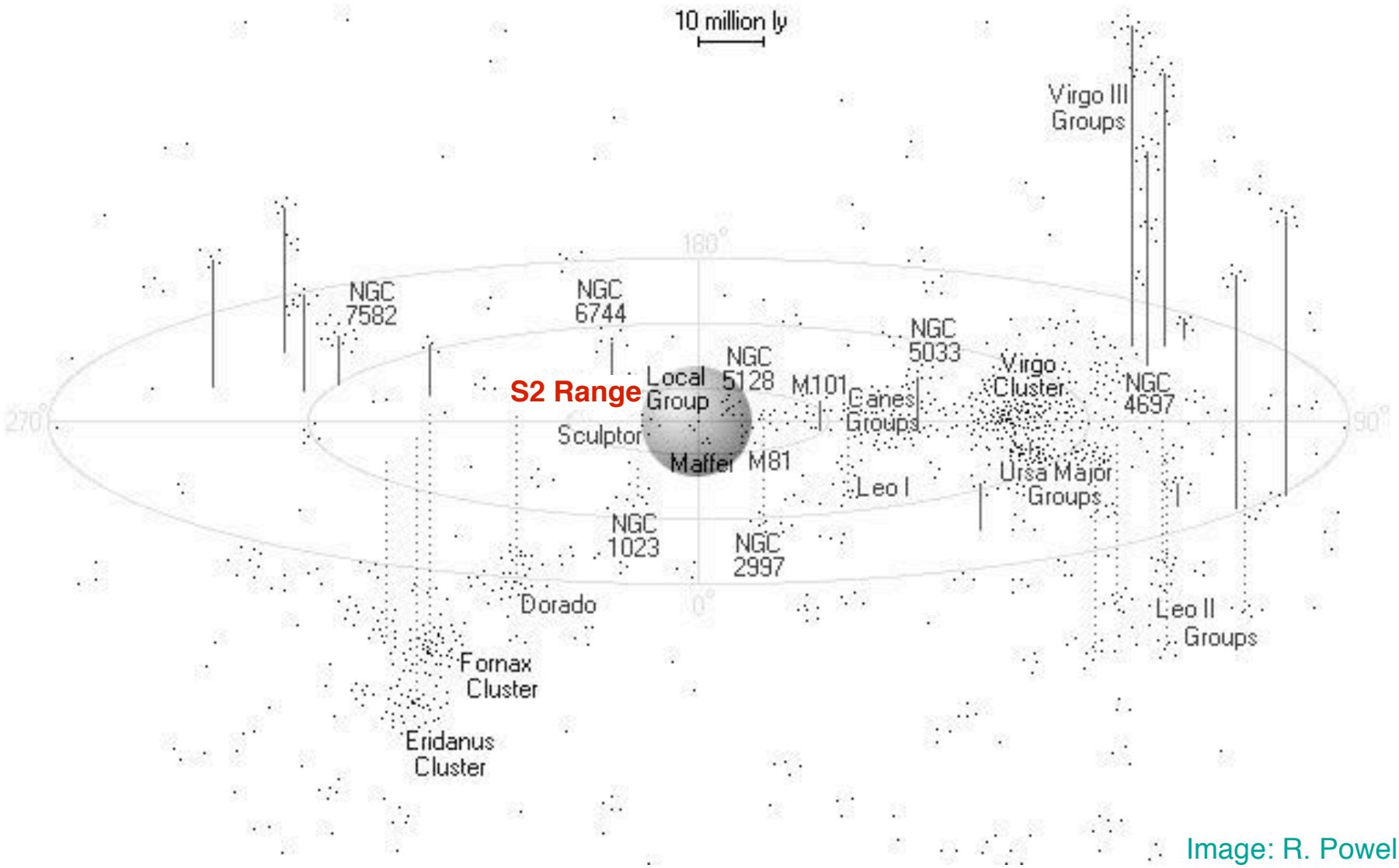

Image: R. Powell

Binary Coalescence Sources & Science:
Binary Neutron Stars: AdLIGO Range

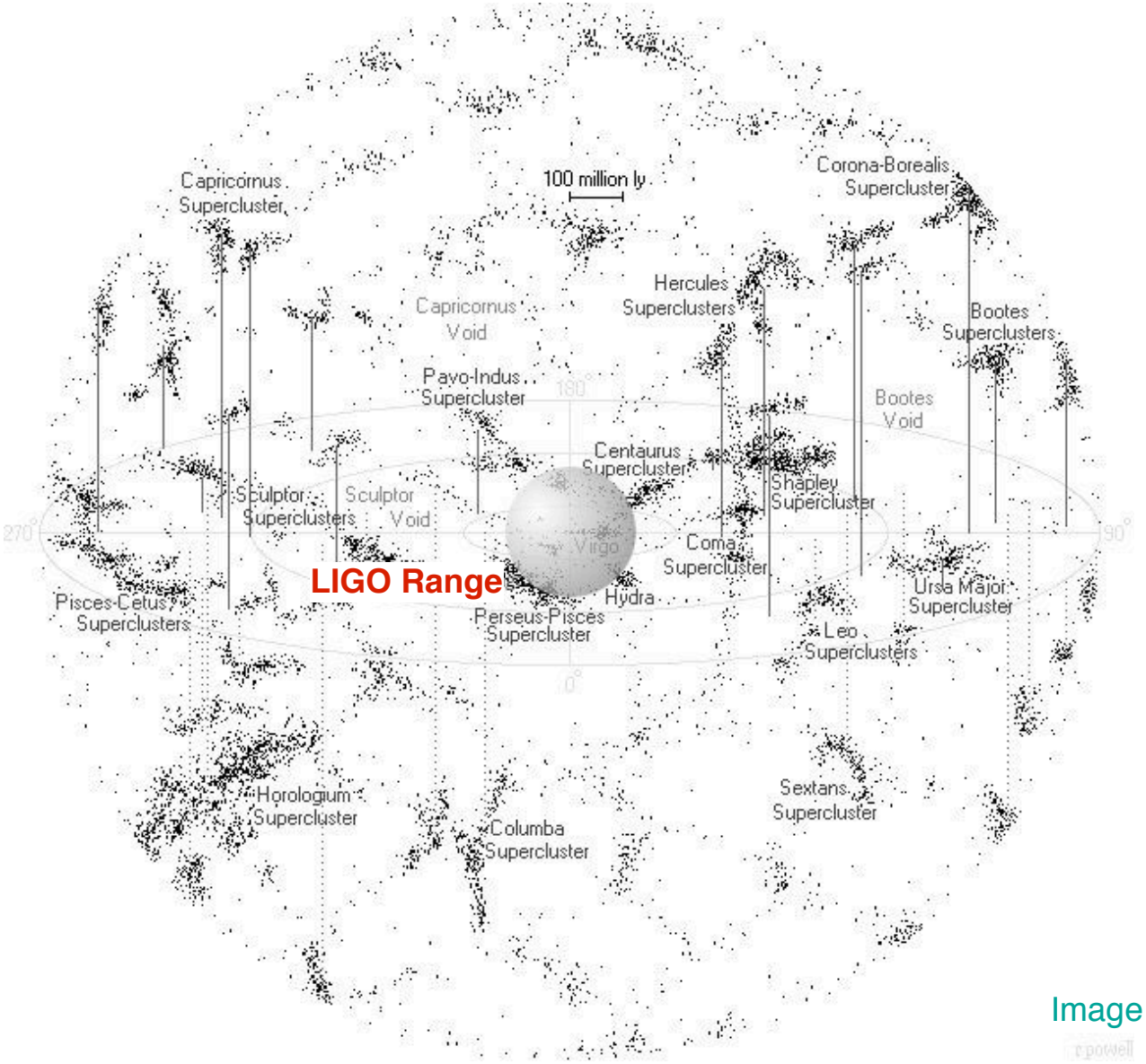

Image: R. Powell

Advanced Interferometer Concept

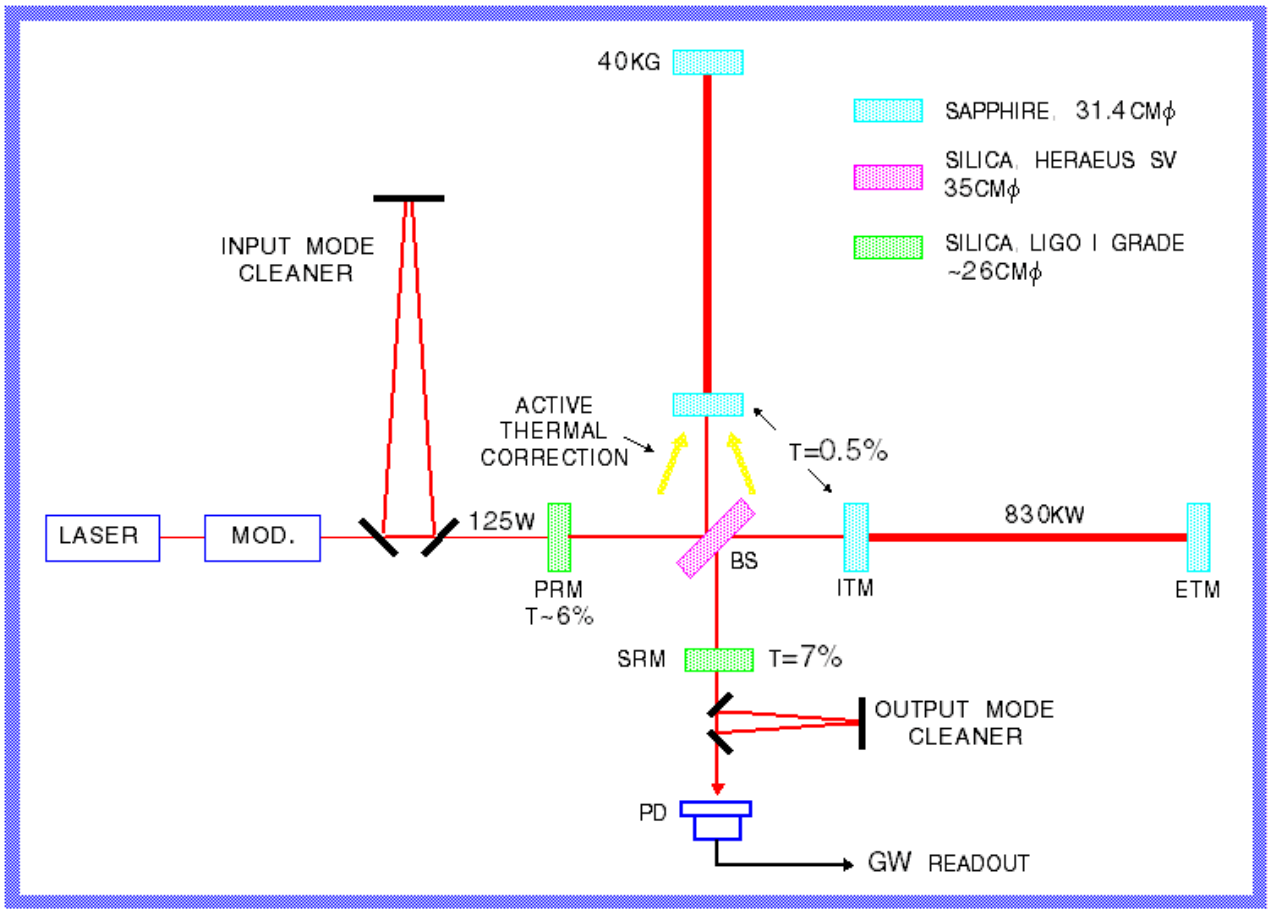

- » Signal recycling
- » 180-watt laser
- » 40 kg Sapphire test masses
- » Larger beam size
- » Quadruple suspensions
- » Active seismic isolation
- » Active thermal correction
- » Output mode cleaner

Projected Performance

- Seismic ‘cutoff’ at 10 Hz
- Suspension thermal noise
- Internal thermal noise
- Unified quantum noise dominates at most frequencies
- ‘technical’ noise (e.g., laser frequency) levels held in general well below these ‘fundamental’ noises

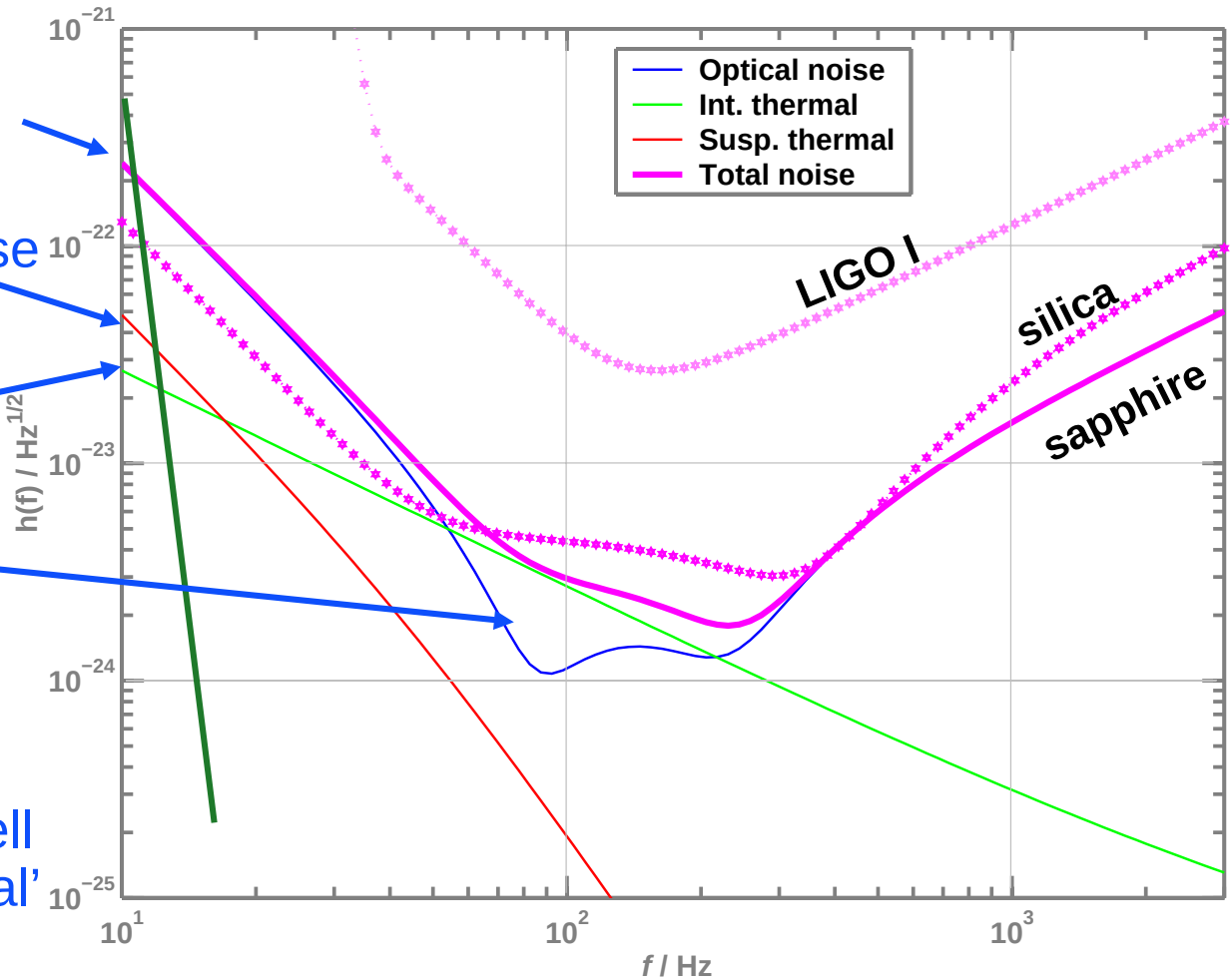

The Gravitational-Wave Spectrum

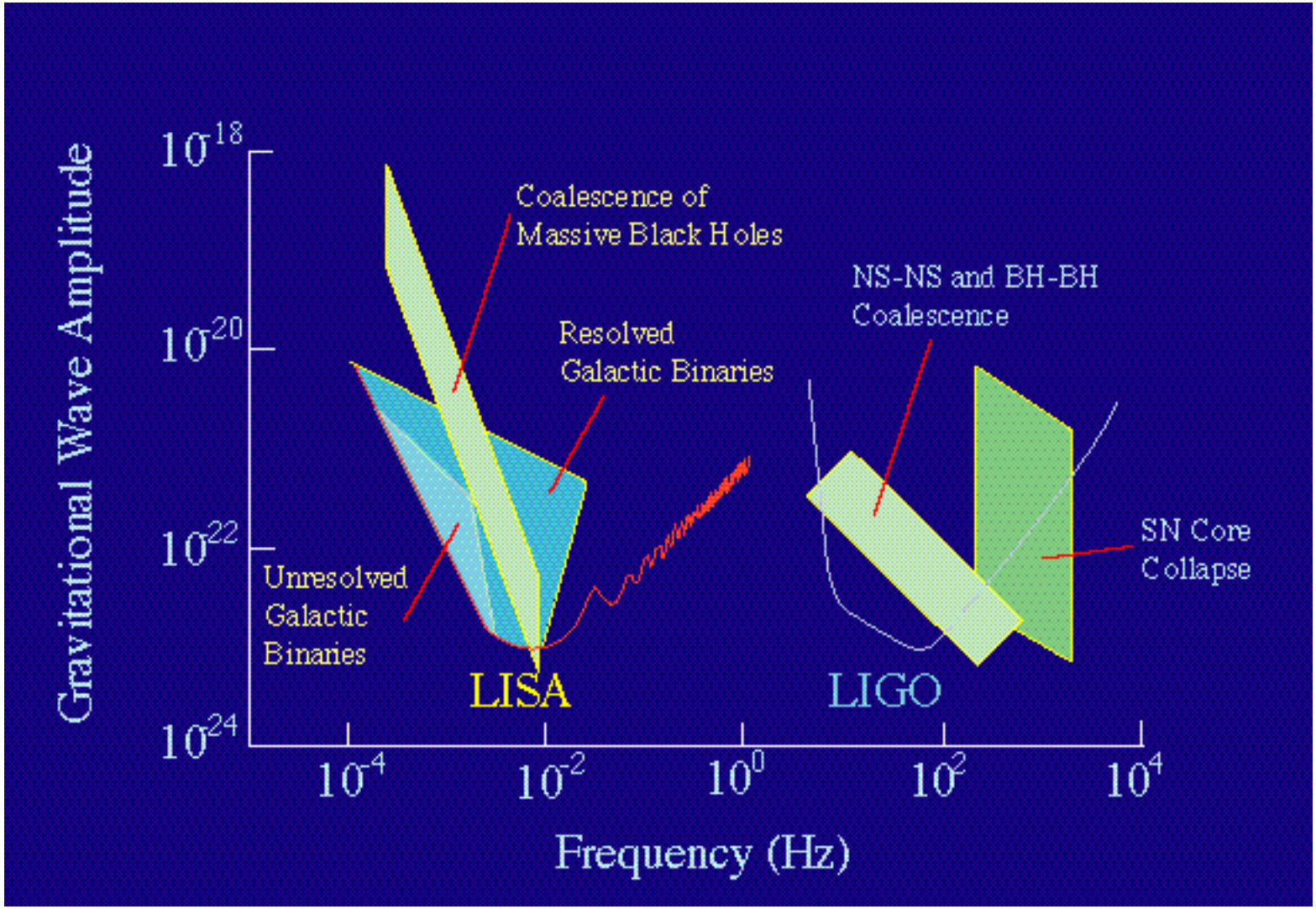

Massive Black Holes in Merging Galaxies

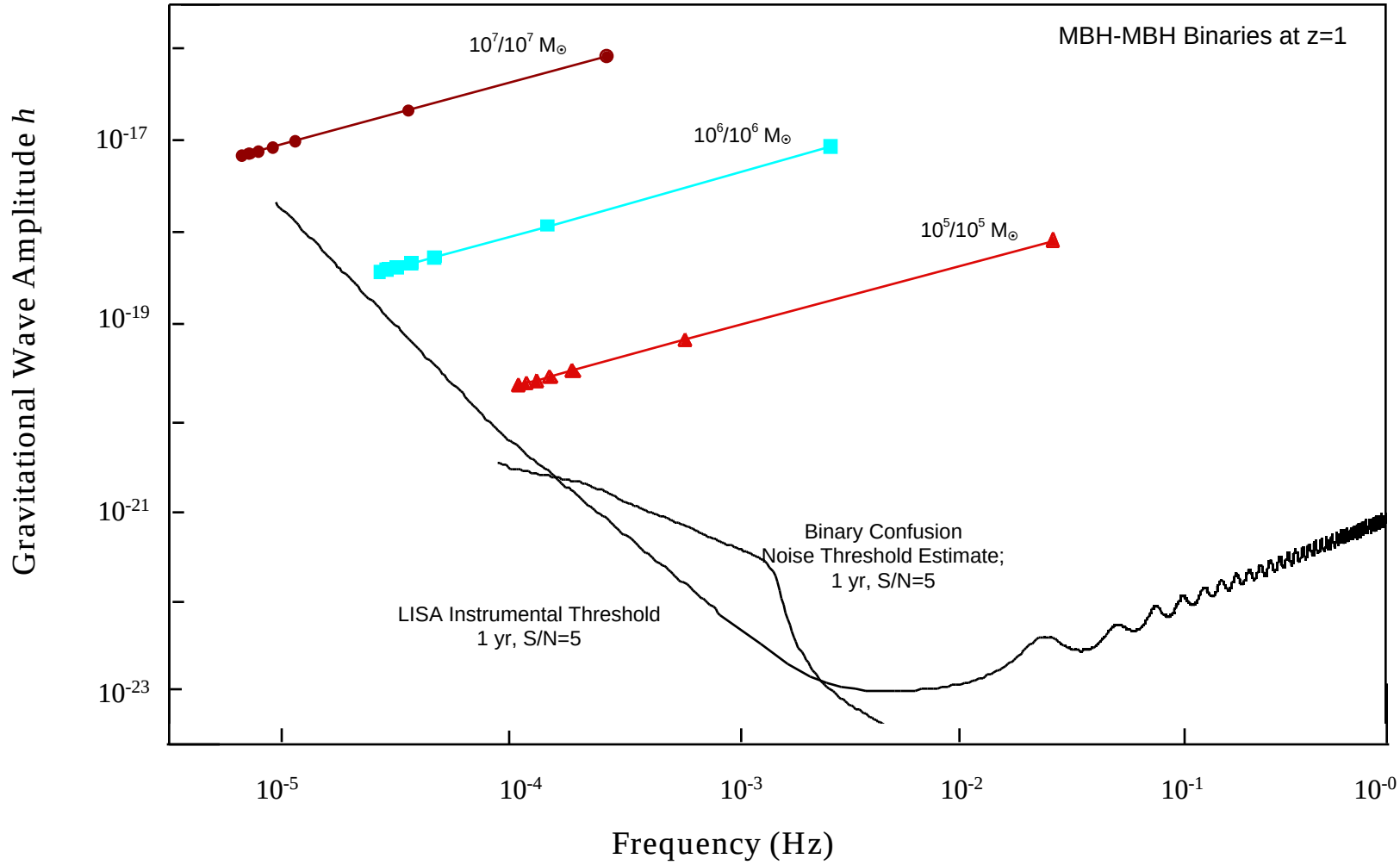

Mission Concept

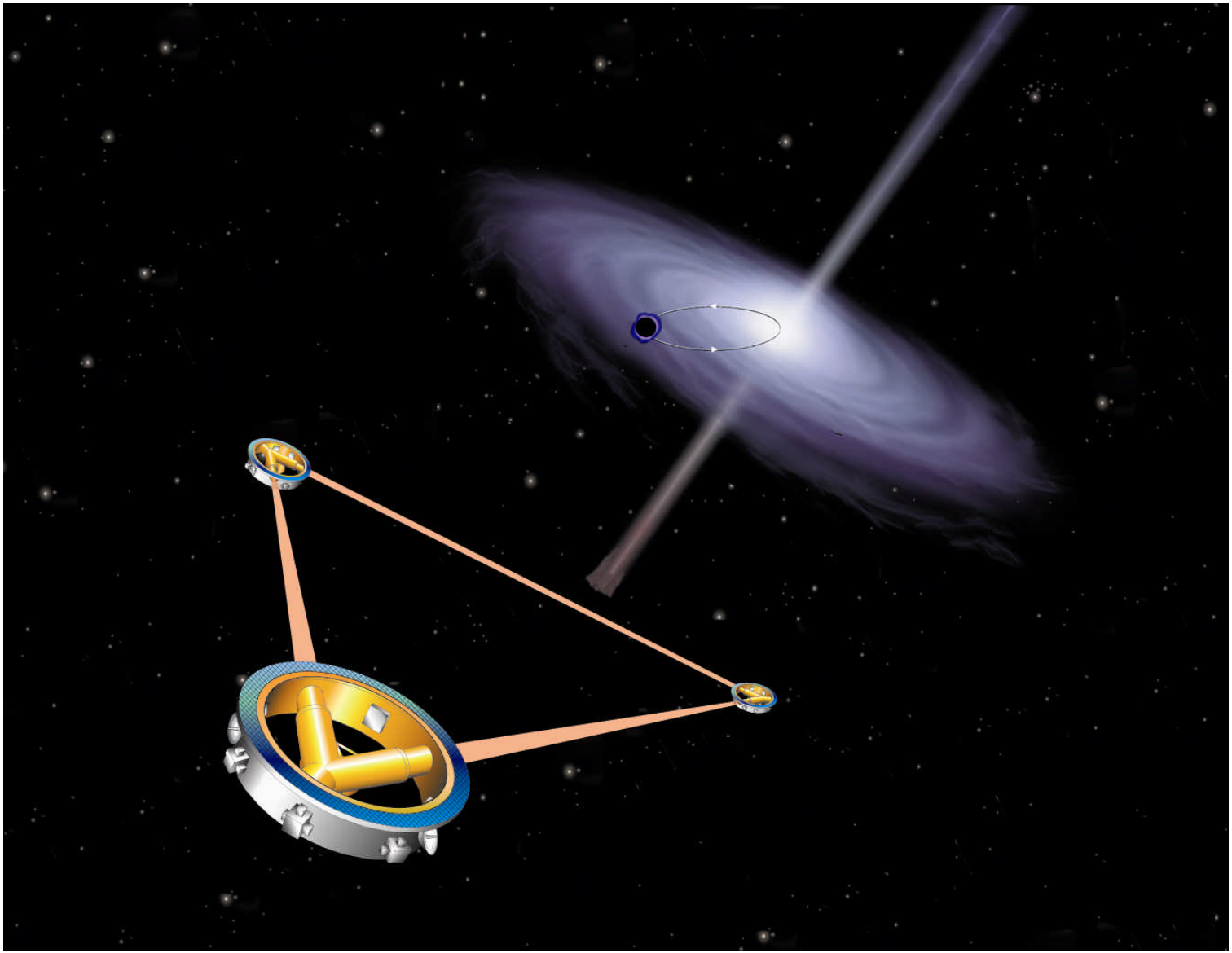

Spacecraft Orbits

- Spacecraft orbits evolve under gravitational forces only
- Spacecraft fly “drag-free” to shield proof masses from non-gravitational forces

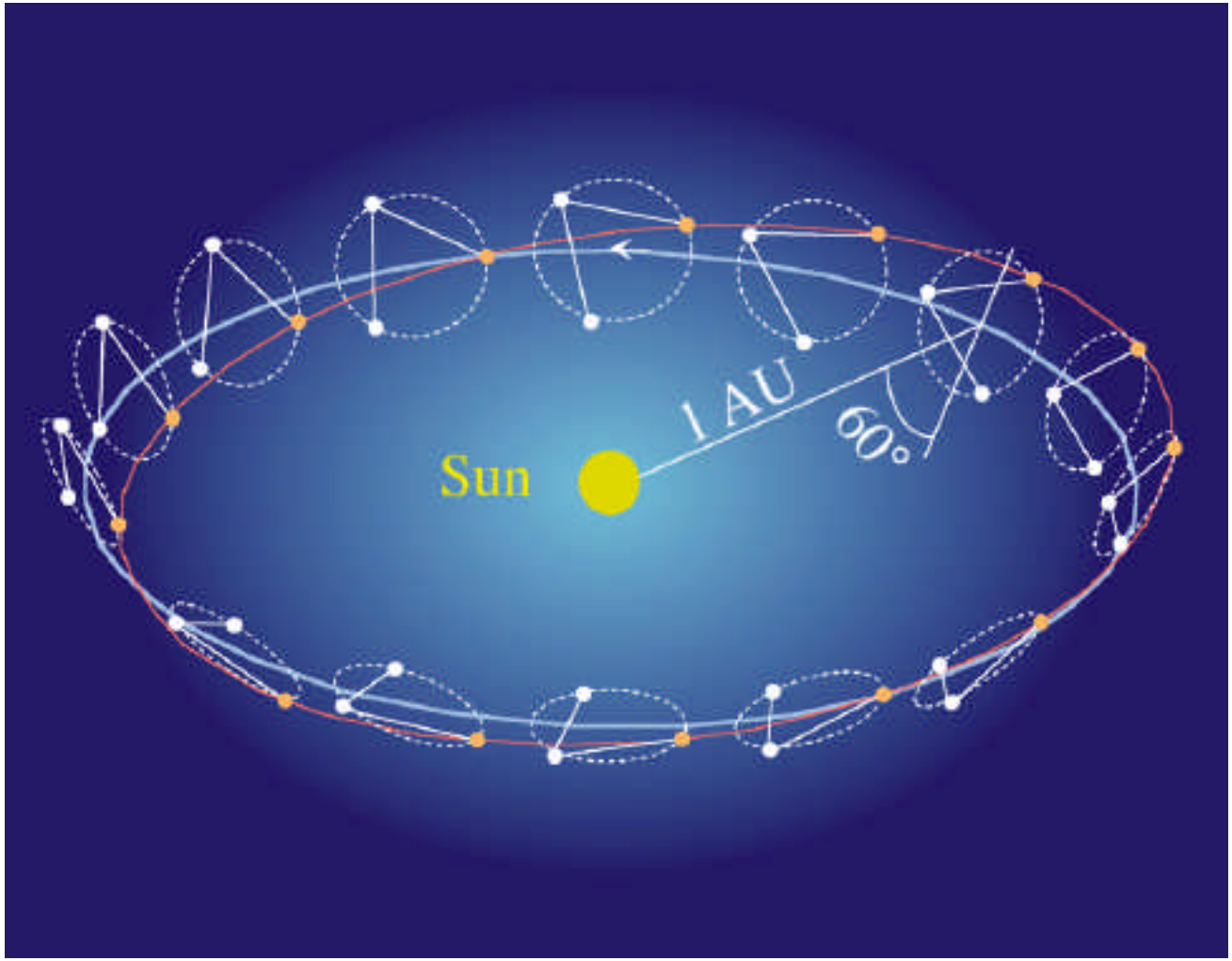

Optical System